
Beam loading in a laser-plasma accelerator using a near-hollow plasma channel

C. B. Schroeder, C. Benedetti, E. Esarey, and W. P. Leemans

Lawrence Berkeley National Laboratory, Berkeley, California 94720, USA

(Dated: 30 December 2013)

Beam loading in laser-plasma accelerators using a near-hollow plasma channel is examined in the linear wake regime. It is shown that, by properly shaping and phasing the witness particle beam, high-gradient acceleration can be achieved with high-efficiency, and without induced energy spread or emittance growth. Both electron and positron beams can be accelerated in this plasma channel geometry. Matched propagation of electron beams can be achieved by the focusing force provided by the channel density. For positron beams, matched propagation can be achieved in a hollow plasma channel with external focusing. The efficiency of energy transfer from the wake to a witness beam is calculated for single ultra-short bunches and bunch trains.

I. INTRODUCTION

Plasma-based accelerators are able to sustain large acceleration gradients, enabling compact accelerating structures. The longitudinal accelerating field of the excited plasma wave can be orders of magnitude greater than conventional accelerators, which are limited by material breakdown. Electron plasma waves with relativistic phase velocities may be excited by the ponderomotive force of an intense laser[1] or the space-charge force of a charged particle beam.[2,3] High-quality 1 GeV electron beams have been produced using intense laser pulses in cm-scale plasmas.[4] Beam-driven plasma waves have also been used to double the energy of a fraction of electrons on the beam tail by the plasma wave excited by the beam head.[5] Plasma-based acceleration of positron beams has also been demonstrated.[6] These experimental successes have resulted in further interest in the development of plasma-based acceleration as a basis for future linear colliders.[7,8]

Hollow plasma channels, with zero density out to the channel radius and constant density for larger radii, have been studied due to the beneficial properties of the accelerating structure.[9–11] In a hollow channel, the transverse profile of the driver is largely decoupled from the transverse profile of the accelerating mode. Furthermore, for a relativistic driver, the accelerating gradient is transversely uniform. In addition, the accelerating mode of the hollow channel is primarily electromagnetic, unlike the electrostatic fields excited in a homogeneous plasma. Development of methods to produce hollow channels is an area of active research.[12]

Recently it has been proposed[13] to use a partially-filled (near-hollow) plasma channel, with plasma density in the channel much less than the plasma density in the channel wall, to provide independent control of the amplitude of the accelerating and focusing forces. The accelerating field is provided by the wall density and the focusing field is determined by the channel density. It was also shown in Ref. 13 that the accelerating and focusing forces in this geometry can mitigate emittance growth from Coulomb collisions with background ions, preserving ultra-low emittance for high-energy physics applications.

In this work we discuss beam-loading of a laser-driven wakefield by a relativistic charged particle beam in a near-hollow plasma channel. Beam-loading has been previously examined in homogeneous plasmas in the linear[14,15] and nonlinear[16] regimes. The different transverse structures of the wakefield excited in a near-hollow channel, compared to a homogeneous

plasma, results in a fundamentally different beam loading limit. For a homogeneous plasma the beam density is limited, whereas, for a near-hollow plasma channel, the beam charge is limited independent of the beam transverse shape or size. We show that, in a near-hollow plasma channel geometry, by properly phasing and shaping an accelerating particle beam, high-gradient acceleration can be achieved with high-efficiency, without induced energy spread or emittance growth. For the case of electron beams, focusing is provided by the plasma density in the channel, while a hollow plasma channel is considered for positron beams with external focusing.

This paper is organized as follows. In Sec. II we discuss the longitudinal wakefields driven by a laser and a particle beam in a near-hollow plasma channel. Throughout this paper wakefield excitation is considered analytically in the linear regime. The condition for laser guiding in the near-hollow plasma channel is calculated in Sec. II A. The accelerated beam current for optimal (i.e., without induced energy spread) beam loading is presented for this plasma channel geometry. The efficiency of energy transfer form the laser-driven wakefield to the witness particle beam is examined. In contrast to the case of a homogeneous plasma, the linear laser-driven wakefield contains both electromagnetic and electrostatic modes, resulting in reduced efficiency. Section III describes control of the focusing forces provided by the channel density, and positron acceleration in a hollow plasma channel is discussed. A summary and conclusions are presented in Sec. IV.

II. ACCELERATING WAKEFIELDS IN A NEAR-HOLLOW PLASMA CHANNEL

Consider a neutral plasma channel with an initial electron plasma density of the form

$$n(r) = \begin{cases} n_c, & r < r_c \\ n_w, & r \geq r_c \end{cases}, \tag{1}$$

where n_w is the electron plasma density in the wall, n_c is the electron plasma density in the channel ($n_c \ll n_w$), and r_c is the channel radius. We will consider channel radii such that $k_w r_c \sim 1$ where $k_w^2 = 4\pi n_w e^2/m_e c^2$ is the plasma wavenumber corresponding to the wall density, with m_e and e the electronic rest mass and charge, respectively, and c is the speed of light in vacuum. To provide weak focusing of an electron beam we will consider $k_c^2 \ll k_w^2$, where $k_c^2 = 4\pi n_c e^2/m_e c^2$ is the plasma wavenumber corresponding to the channel density.

An intense laser propagating in the channel will drive surface currents in the channel walls exciting a wakefield. The transerse ponderomotive force of the laser will also expel electrons radially out of the channel, leaving the background ion density remaining in the channel. The expelled channel electrons do not return since the space charge force of the channel ions is screened by the plasma electrons in the wall. The condition for expulsion[1] of channel electrons is $a_0^2/(1+a_0^2/2)^{1/2} > k_c^2 w_0^2/2$, where $a_0^2 \simeq 7.32\times 10^{-19}\lambda_0^2[\mu\mathrm{m}]I_0[\mathrm{W/cm^2}]$ with λ_0 the laser wavelength, I_0 the peak laser intensity, and w_0 the laser spot size. This condition is well-satisfied for relativistic laser intensities $a_0 \sim 1$ and guided laser pulses $w_0 \sim k_w^{-1}$ in a near-hollow plasma channel. A charged particle beam with density $n_b \sim n_w \gg n_c$ may also expel channel electrons. In the limit of a near-hollow plasma channel $k_c^2 \ll k_w^2$, the accelerating field will be determined by the wall density $E_z \sim E_w$, where $E_w = m_e c^2 k_w/e$. The ion density in the channel will provide a transverse electrostatic field, and the focusing force on a relativistic beam will be determined by the channel density, $E_r - B_\theta \simeq E_c k_c r/2$, where $E_c = m_e c^2 k_c/e$. A detailed calculation of the wakefields in this plasma geometry is presented in the Appendix.

A. Laser-driven wakefield

The wake excited inside such a channel will consist of an electromagnetic wake owing to surface currents driven in the channel walls and fields owing to the background ions in the channel. For a sharp channel-wall interface, electrostatic wakefields excited outside the channel will not couple to channel modes.[17]

The wakefield excited by the laser can be derived from Maxwell equations and the linearized fluid equations for a cold, collisionless plasma, assuming a quasi-static driver.[1] A derivation of the linear wakefields is presented in the Appendix valid for $|E_z| < E_w$. In the limit $k_c^2 \ll k_w^2$, the accelerating field inside the channel is dominated by the currents in the wall and has the form[9]

$$E_{zL}/E_w = -\Omega^2 \int_\infty^\zeta d\zeta' \cos[\Omega(\zeta-\zeta')]a^2(r=r_c,\zeta')/4, \tag{2}$$

to order $a^2(r_c) < 1$, where $a(r,\zeta) = eA/m_e c^2$ is the normalized transverse vector potential profile of the laser, $\zeta = z - \beta_p t$, $c\beta_p$ is the driver velocity, and $\gamma_p = (1-\beta_p^2)^{-1/2} \gg 1$. The length scales are normalized to the skin depth of the wall k_w^{-1}. For a laser driver,

$\gamma_p \sim k_0/k_w = 2\pi/(k_w\lambda_0)$, where λ_0 is the laser wavelength. The electromagnetic channel mode wavenumber[9,11] is $k_w\Omega$, with

$$\Omega = \left[1 + \frac{r_c K_0(r_c)}{2K_1(r_c)}\right]^{-1/2}. \tag{3}$$

For example, $\Omega \simeq 0.8$ for $r_c = 1.5$. For a bi-Gaussian laser profile with envelope

$$a^2 = a_0^2 \exp(-\zeta^2/2L^2)\exp(-2r^2/w_0^2), \tag{4}$$

where L is the rms intensity pulse length and w_0 the laser spot size, the wake amplitude behind the laser $E_{zL}/E_w = \hat{E}_L \cos(\Omega\zeta + \varphi)$, where φ is a constant phase determined by the driver, is

$$|\hat{E}_L| = E_{\rm peak}/E_w = a_0^2(\pi/8)^{1/2}\Omega^2 L e^{-(\Omega L)^2/2} e^{-2r_c^2/w_0^2}. \tag{5}$$

For a Gaussian longitudinal laser profile, the wake amplitude is maximum for $\Omega L = 1$, and $E_{\rm peak}/E_w \simeq 0.38\Omega a_0^2 \exp(-2r_c^2/w_0^2)$.

A laser pulse can be guided in a near-hollow channel. The condition for quasi-matched propagation (i.e., without evolution in the transverse second moment of the laser intensity) in the channel for relativistic intensities $a_0 \sim 1$ can be calculated following Ref. 18. Guiding for a transversely Gaussian laser pulse is provided when the laser spot satisfies[18]

$$\int_0^\infty dr 2r\rho\left(2r^2/w_0^2 - 1\right) e^{-2r^2/w_0^2} = 1, \tag{6}$$

where $\rho = n/(n_0\gamma)$ is the proper density. Substituting Eq. (1) for ρ (i.e., neglecting guiding contributions from the wakefield and self-focusing of the laser in the plasma) yields

$$w_0 = r_c/[\ln(r_c)]^{1/2}. \tag{7}$$

Using Eq. (7) for the matched spot size implies the wake amplitude scales as $|\hat{E}_L| \propto a_0^2 \exp(-2r_c^2/w_0^2) = a_0^2/r_c^2$.

Equation (7) is valid in the low intensity limit ($a_0 < 1$) and for laser powers below the critical power (in the plasma wall). Wakefield and relativistic self-focusing effects can be included in the proper density ρ and the nonlinear integral equation Eq. (6) solved numerically. Figure 1 shows the laser spot size for matched propoagation in a near-hollow channel versus channel radius. The points are the solution to Eq. (6) including the self-consistent wakefield and plasma motion excited by a bi-Gaussian ($L = 1$) laser with $a_0 = 0.8$

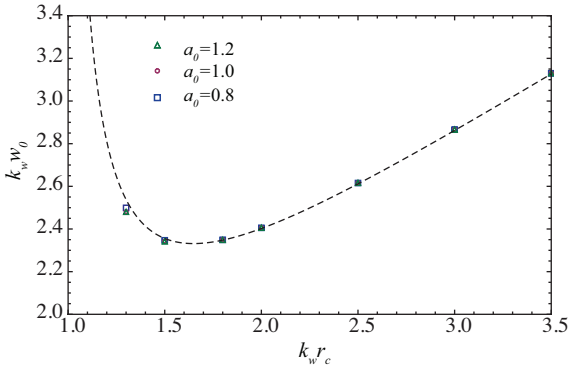

FIG. 1. (color online) The laser spot size $k_w w_0$ for matched propoagation in a near-hollow channel versus channel radius $k_w r_c$: The points are the solution to Eq. (6) including the self-consistent wakefield and plasma motion for a bi-Gaussian ($L = 1$) laser with $a_0 = 0.8$ (blue squares), $a_0 = 1.0$ (red circles), and $a_0 = 1.2$ (green triangles). The dashed curve is Eq. (7), $w_0 = r_c/[\ln(r_c)]^{1/2}$.

(blue squares), $a_0 = 1.0$ (red circles), and $a_0 = 1.2$ (green triangles). The dashed curve in Fig. 1 is Eq. (7). Figure 1 shows that Eq. (7) is an excellent approximation to the guiding condition in the regime of quasi-linear laser wakefield excitation $a_0 \sim 1$.

B. Beam-driven wakefield

The space-charge forces of a relativistic charged particle beam propagating along the axis of the channel will also excite plasma wakefields. A calculation of the particle beam driven wakefields derived from the Maxwell equations and linearized cold fluid equations, assuming the quasi-static approximation, is presented in the Appendix. In the limit $k_c^2 \ll k_w^2$, the accelerating field in the channel driven by a charged particle beam is dominated by the electromagnetic mode and has the form[11]

$$E_{zb}/E_w = W_0 \Omega^2 \int_\infty^\zeta d\zeta' \cos[\Omega(\zeta - \zeta')] I(\zeta')/I_A, \tag{8}$$

assuming $E_{zb} < E_w$, where I is the particle beam current, $I_A = m_e c^3/e$ is the Alfvén current, and

$$W_0 = \frac{2K_0(r_c)}{r_c K_1(r_c)}. \tag{9}$$

For example, $W_0 \simeq 1.03$ for $r_c = 1.5$. A witness charged particle beam will be accelerated by the total wakefield generated by the driver (laser or beam) and the witness beam.

C. Beam loading

Van der Meer[14] first considered shaping of the witness beam to eliminate energy spread in a plasma accelerator. Consider a linearly ramped current distribution of length L_b, $I = (1 + \zeta/L_b)I_b$ for $-L_b \leq \zeta \leq 0$, with the bunch head at $\zeta = 0$. For this ramped current distribution solving Eq. (8) yields

$$E_{zb}/E_w = \{[1 - \cos(\Omega\zeta)]/L_b + \Omega \sin(\Omega\zeta)\} W_0 I_b/I_A, \tag{10}$$

within the region of the beam $-L_b \leq \zeta \leq 0$. If we consider a laser-driven wakefield accelerating the particle beam, the total longitudinal field experienced by the beam is $E_z = E_{zL} + E_{zb}$. This ramped current distribution can be used to generate a constant accelerating gradient throughout a bunch, which, consequently, implies zero induced energy spread. A constant gradient throughout a beam of $E_z/E_w = \hat{E}_L \cos(\varphi)$ can be achieved with a beam of length $L_b = \tan(\varphi)/\Omega$ using a peak beam current $I_b/I_A = \hat{E}_L \sin(\varphi)/(W_0\Omega)$, where the peak of the unloaded accelerating field is at $\zeta = 0$ and $\varphi = \Omega\zeta_{\rm head}$ is the phase position of the head of the beam.

The beam charge that can be accelerated is

$$N_b = \hat{E}_L \frac{\tan(\varphi)\sin(\varphi)}{2W_0\Omega^2 k_w r_e}, \tag{11}$$

where $r_e = e^2/m_e c^2$. Note that, for fixed normalized accelerating field amplitude $\hat{E}_L$, the number of particles that can be accelerated in the plasma wakefield increases for decreasing plasma density in the wall, $N_b \propto k_w^{-1} \propto n_w^{-1/2}$. Although this density scaling is similar to that found in a homogeneous plasma,[15] the beam loading limit in a near-hollow plasma channel is fundamentally different than that in a homogeneous plasma. In a homogeneous plasma in the linear regime, beam-loading limits the particle beam density (i.e., more charge may be accelerated with a larger beam transverse size), whereas in a near-hollow plasma channel, Eq. (11) is a limit on the total particle beam charge (independent of transverse beam size).

Figure 2(a) shows an example of a accelerating wakefield E_{zL}/E_w (black curve) driven by a laser with $a_0 = 1.2$, $w_0 = 2.3$, and a sine-longitudinal profile of length $L_s = 3.95$, in a near-hollow plasma channel with radius $r_c = 1.5$ and $n_c/n_w = 5 \times 10^{-5}$. A ramped triangular electron beam is phased with the beam head at $\varphi = \pi/3$, with respect to the

maximum accelerating field (at $\zeta = -4.45$), having peak current $I_b/I_A \simeq 1.1\hat{E}_L$, beam length $L_b = \sqrt{3}/\Omega \simeq 2.18$, and beam radius $\sigma_r = 0.25$. Figure 2 was generated using the particle-in-cell code `INF&RNO`.[19] The wakefield from the beam modifies the total wakefield [red curve in Fig. 2(a)] such that the beam experiences a constant accelerating field ($E_z = -|\hat{E}_L|/2$) throughout the beam. These quantities have been normalized such that they are independent of the wall density. Operating at a wall density of $n_w = 10^{17}$ cm^{-3} for this example would yield a constant accelerating gradient of 2.3 GV/m throughout the beam, a wakefield wavelength of 132 μm, a beam charge of 167 pC, a beam length of 36 μm (rms length 15 μm), and a channel radius of 25 μm. As this example shows, high-gradient accelerating fields can be achieved without induced energy spread in a near-hollow plasma channel geometry.

1. Beam loading efficiency

The laser-driven wakefield excites an electromagnetic mode, driven by surface current in the channel wall and an electrostatic mode both in the channel $r < r_c$ and in the wall $r > r_c$. If we assume a near-hollow channel such that $n_c/n_w \ll a^2(r = r_c)/a^2(r = 0)$, then the energy deposited in the electrostatic channel mode may be neglected compared to the electromagnetic channel mode. The initial energy deposited in the plasma channel by the laser-driver is $U_i = U_{\rm em} + U_{\rm es}$, where $U_{\rm em}$ and $U_{\rm es}$ is the total energy per unit length in the electromagnetic and electrostatic modes, respectively, given by Eqs. (A24) and (A31). For an optimally shaped bunch to eliminate the energy spread, the peak field following the bunch is reduced by $\cos(\varphi)$, where $\varphi = \Omega\zeta_{\rm head}$ is the phase position of the head of the beam. Since the relativistic witness beam only excites an electromagnetic mode, the final energy in the plasma channel after the beam-plasma interaction is $U_f = U_{\rm em}\cos^2(\varphi) + U_{\rm es}$.

The efficiency of energy transfer from the laser-driven electromagnetic wakefield to the witness particle beam is

$$\eta = 1 - \frac{U_f}{U_i} = \frac{\sin^2(\varphi)}{1 + U_{\rm es}/U_{\rm em}}. \tag{12}$$

In general, with no wake-induced energy spread, there is a trade-off between efficiency η and accelerating gradient $\hat{E}_{zL}\cos(\varphi)$. The energy in the electrostatic mode does not couple to the witness particle beam and reduces the overall efficiency. Using (A24) and (A31), the ratio of energy deposited in the electrostatic to electromagnetic modes in the plasma channel

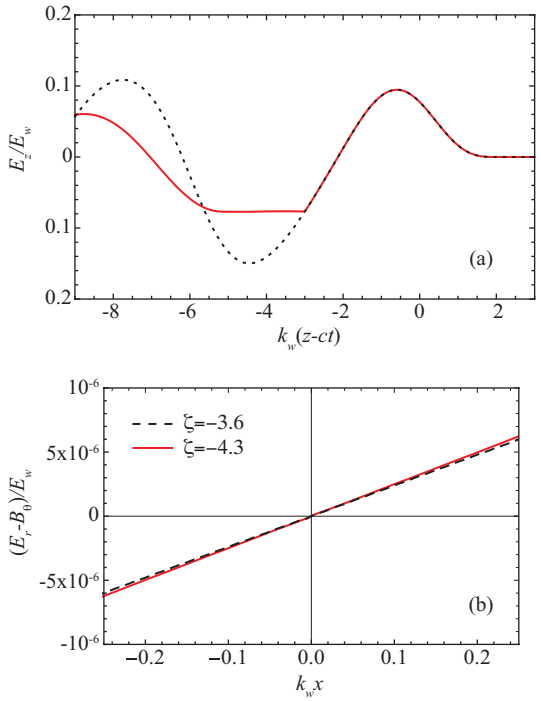

FIG. 2. (color online) (a) Normalized accelerating wakefield E_z/E_w versus ζ with (red solid curve) and without (black dotted curve) witness electron beam. Plasma channel has parameters $r_c = 1.5$ and $n_c/n_w = 5 \times 10^{-5}$. Wakefield is driven by a laser pulse with $a_0 = 1.2$, $w_0 = 2.3$, and sine-longitudinal profile of length length $L_s = 3.95$. Witness electron beam is phased $\varphi = \pi/3$, with $I_b/I_A \simeq 1.1\hat{E}_L$, $L_b = \sqrt{3}/\Omega \simeq 2.18$, $\sigma_r = 0.25$, $\gamma = 10^4$, and $\epsilon_n = 0.03$. (b) Normalized transverse wakefield $(E_r - B_\theta)/E_w$ versus transverse position x $(y = 0)$ inside the beam at two phases $\zeta = -3.6$ (dashed black line) and $\zeta = -4.3$ (solid red line).

is

$$\frac{U_{\rm es}}{U_{\rm em}} = \frac{A_1^2}{A_0^2}\left(\frac{\Omega^2 K_0(r_c)}{r_c K_1(r_c)}\right)\int_{r_c}^{\infty} r dr\left\{\left[\frac{a^2(r)}{a^2(r_c)} - \frac{K_0(r)}{K_0(r_c)}\right]^2 + \left[\frac{\partial_r a^2(r)}{a^2(r_c)} + \frac{K_1(r)}{K_0(r_c)}\right]^2\right\}, \qquad (13)$$

assuming $k_c \ll k_w$. Note that, for a laser with transverse profile $a^2(r) = a^2(r_c)K_0(r)/K_0(r_c)$ in the wall plasma, the laser will only couple to the electromagnetic mode, $U_{\rm es} = 0$, yielding higher overall efficiency. For a bi-Gaussian laser driver, Eq. (4), resonant with the electromagnetic mode ($\Omega L = 1$), the ratio of energy deposited in the electrostatic to electromagnetic modes in the plasma channel is, with $k_c \ll k_w$,

$$\frac{U_{\rm es}}{U_{\rm em}} = \frac{e^{(1-\Omega^{-2})}K_0(r_c)}{\Omega^2 r_c K_1(r_c)}\int_{r_c}^{\infty} r dr\left\{\left[e^{-2(r^2-r_c^2)/w_0^2} - \frac{K_0(r)}{K_0(r_c)}\right]^2 + \left[\frac{K_1(r)}{K_0(r_c)} - \frac{4r}{w_0^2}e^{-2(r^2-r_c^2)/w_0^2}\right]^2\right\}. \qquad (14)$$

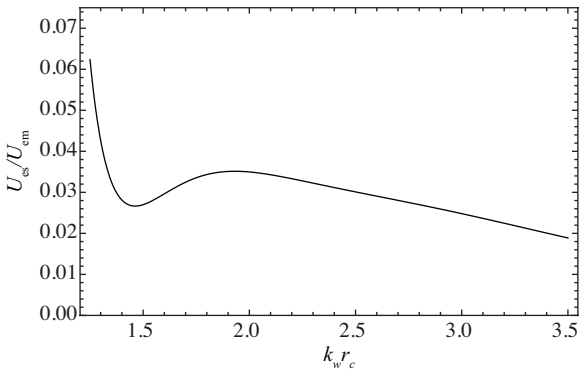

FIG. 3. Ratio of energy per unit length in the electrostatic mode to that in the electromagnetic mode deposited in a plasma channel by a bi-Gaussian laser driver with duration $L = \Omega^{-1}$ and spot size $w_0 = r_c/\sqrt{\ln(r_c)}$ (quasi-matched propagation in the plasma channel).

Figure 3 plots $U_{\rm es}/U_{\rm em}$ versus channel radius r_c, assuming the relation $w_0 = r_c/\sqrt{\ln(r_c)}$ for quasi-matched propagation[18] in the low intensity, low power limit. For typical parameters, the energy in the electrostatic mode is a few percent of the total energy deposited in the plasma channel. For the parameters of Fig. 2, the overall efficiency of energy transfer from laser-driven wakefield to beam is $\eta \simeq 73\%$.

2. Beam loading with short beams

Shorter beams may be required for various applications. For example, ultra-short beams may be used for dynamical studies in ultrafast science. For high-energy physics applications, short beams can be effective in suppressing beamstrahlung effects.[8] If a shorter duration beam is desired one can consider a trapezoidal current distribution:

$$\frac{I}{I_A} = \hat{E}_L \frac{\sin(\varphi)}{W_0 \Omega} \left(1 + \frac{\Omega\zeta}{\tan(\varphi)}\right) \Theta(-\zeta + L_b), \tag{15}$$

for $\zeta < 0$, where $\Theta(x) = 1$ for $x > 0$ and zero otherwise, and the beam length is $L_b \leq \tan(\varphi)/\Omega$. For the beam distribution given by Eq. (15) the field experienced by the beam is constant throughout the beam with amplitude $E_z/E_w = \hat{E}_L \cos(\varphi)$, and the total number of particles in the beam is

$$N_b = L_b \left[1 - \frac{\Omega L_b}{2\tan(\varphi)}\right] \frac{\sin(\varphi)}{W_0 \Omega} \frac{|\hat{E}_L|}{k_w r_e}. \tag{16}$$

Note that Eq. (16) is independent of the transverse size and shape of the witness particle beam.

With a trapezoidal beam, the back of the particle beam generates a wake (depositing energy back into the plasma), and hence the overall efficiency is reduced. The efficiency of energy transfer from the wakefield to the beam using a trapezoidal current distribution is $\eta = \eta_c(1 + U_{\rm es}/U_{\rm em})^{-1}$, with

$$\eta_c = \Omega L_b \cos(\varphi) \left[2\sin(\varphi) - \Omega L_b \cos(\varphi)\right]. \tag{17}$$

In the limit of the triangular beam, $L_b = \tan(\varphi)/\Omega$, the efficiency is maximized $\eta = (1 + U_{\rm es}/U_{\rm em})^{-1} \sin^2(\varphi)$. For fixed beam length L_b, the optimal phase for maximum efficiency is

$$\varphi = \arctan\left[\Omega L_b/2 + \sqrt{1 + (\Omega L_b/2)^2}\right]. \tag{18}$$

In the limit of ultra-short bunches $L_b \ll 1$, the optimal phase for efficiency is $\varphi \simeq \pi/4 + \Omega L_b/4$, with the efficiency $\eta \simeq \Omega L_b(1 + U_{\rm es}/U_{\rm em})^{-1}$.

3. Bunch trains

Higher efficiency of energy transfer from the wakefield to the beam can be achieved for short bunches ($L_b \ll 1$) by using multiple bunch trains. As an example, consider two short trapezoidal bunches. The first bunch of length $L_1 \ll 1$ with its head located at the phase φ_1 experiences a uniform accelerating field amplitude $E_L \cos(\varphi_1)$ throughout the bunch, with charge N_{b1} given by Eq. (16) and efficiency η_{c1} given by Eq. (17). A second bunch can be phased behind the first bunch (with head at φ_2 with respect to the peak of the wakefield of a trailing plasma wave bucket behind the first bunch) such that the accelerating gradient is equal throughout both bunches, which implies $\varphi_2 = \arccos[\cos(\varphi_1)/\sqrt{1 - \eta_{c1}}] < \varphi_1$. The second bunch length $L_2 > L_1$ can be chosen such that the charge in both bunches is equal $N_{b2} = N_{b1}$. In this way, the efficiency (beam charge) is doubled, maintaining a constant accelerating gradient (in both bunches), while using ultra-short bunches $1 \gg L_2 > L_1$. For example, assuming $r_c = 1.5$, if the head of the first trapezoidal bunch is phased at $\varphi_1 = \pi/4$, with accelerating field $E_L/\sqrt{2}$ and bunch length $L_1 = 0.1$, then the efficiency is $\eta_{c1} = 0.0764$. The amplitude of the laser-driven wakefield following the bunch is reduced $(1 - \eta_{c1})^{1/2} E_L \simeq 0.961 E_L$. A second trapezoidal bunch can be placed in a bucket trailing the first with phase $\varphi_2 \simeq 0.744$ (with respect to the local peak) such that the accelerating field amplitude is $0.707 E_L$ throughout the bunch, and the length is $L_2 = 0.110$ such that

the bunch charge is equal $N_{b2} = N_{b1}$. The total efficiency of energy transfer is twice that of the single bunch.

In a similar fashion, additional trapezoidal bunches can be added to the train to further increase the efficiency. The m^{th} bunch in the train should be phased, with respect to the local wakefield peak,

$$\varphi_m = \arccos\left[\frac{\cos(\varphi_1)}{\sqrt{1-(m-1)\eta_{c1}}}\right] < \varphi_{m-1}, \tag{19}$$

where $\eta_{c1} = \eta_c(\varphi_1, L_1)$ is given by Eq. (17). The bunch length to maintain equal charge is $L_{m-1} < L_m$ with

$$L_m = \Omega^{-1}\tan(\varphi_m)\left[1 - \sqrt{1 - \frac{2\Omega L_1 \sin(\varphi_1)\cos(\varphi_m)}{\sin^2(\varphi_m)\sqrt{1-(m-1)\eta_{c1}}}\left(1 - \frac{\Omega L_1}{2\tan(\varphi_1)}\right)}\right]. \tag{20}$$

Here a constant gradient will be maintained throughout all the bunches of equal charge. The total efficiency after m bunches is

$$\eta_{\text{total}} = m\eta_{c1}\left(1 + U_{\text{es}}/U_{\text{em}}\right)^{-1}, \tag{21}$$

where $U_{\text{es}}/U_{\text{em}}$ is given by Eq. (13) and determined by the driver.

The limit on the number of bunches (with equal charge, experiencing equal acceleration) will be set when the wakefield amplitude becomes sufficiently reduced (energy transferred to the bunch train) such that a uniform accelerating gradient can not be achieved for the bunch charge. The efficiency using a m-bunch train can approach that of a single beam Eq. (12) with the number of bunches equal to the largest previous integer of $\sin^2(\varphi)/\eta_{c1}$. In the above example ($L_1 = 0.1$ and $\varphi_1 = \pi/4$), six bunches (with lengths $\leq L_6 \simeq 0.248$) could be used with constant accelerating gradient of $E_L\cos(\pi/4)$ and an overall efficiency of $6\eta_{c1}/(1 + U_{\text{es}}/U_{\text{em}})$.

III. TRANSVERSE WAKEFIELDS IN A NEAR-HOLLOW PLASMA CHANNEL

In a near-hollow plasma channel the focusing force provided by the electromagnetic mode driven by currents in the wall is reduced for relativistic drivers owing to the near cancellation (to order $\sim \gamma_p^{-2}$) of the transverse fields in the Lorentz force. Hence, one can consider

operating in a regime where the plasma density in the channel dominates and provides a constant, uniform focusing force. The laser, satisfying $a_0^2/(1+a_0^2/2)^{1/2} > k_c^2 w_0^2/2$, and the witness beam, with beam density n_b typically satisfying $n_b \sim n_w \gg n_c$, will expel any electrons in the low density channel, forming an ion column. The focusing wakefield excited in the channel is then [to order $a^2(r_c) < 1$ in the laser field]

$$(E_r - \beta B_\theta)/E_w = (E_c/E_w)k_c r/2 - \frac{r}{16\gamma_p^2}\left(1+\frac{\gamma_p^2}{\gamma^2}\right)\Omega^3 \int_\infty^\zeta d\zeta' \sin[\Omega(\zeta-\zeta')]a^2(r=r_c,\zeta') + \frac{r}{2\gamma^2} W_0 \Omega^3 \int_\infty^\zeta d\zeta' \sin[\Omega(\zeta-\zeta')] I(\zeta')/I_A, \quad (22)$$

where $\gamma^2 = 1/(1-\beta^2) \gg 1$ and $c\beta$ is the witness beam velocity. The first term on the right-hand side of Eq. (22) is due to the ions in the channel, the second term is due to the electromagnetic mode excited in the walls for a laser driver, and the third term is the self wakefield driven by the witness beam. The focusing wakefield is linear with respect to radial position and, hence, the normalized transverse slice emittance will be preserved.

The ion density in the channel can be used as an effective method to control the focusing force on a relativistic electron beam. In the regime $\gamma^2 \gg \gamma_p^2$ and $n_c/n_w \gg a_0^2(r=r_c)/(8\gamma_p^2)$, the focusing from the channel ion density dominates and

$$E_r - \beta B_\theta \simeq E_c k_c r/2, \quad (23)$$

yielding $k_\beta = k_c/\sqrt{2\gamma}$, where k_β is the betatron wavenumber for the focusing force. In this regime matched propagation for an electron beam is achieved for

$$\frac{n_c}{n_w} = \frac{2\epsilon_n^2}{\gamma \sigma_r^4}, \quad (24)$$

where ϵ_n is the rms normalized transverse emittance and σ_r is the rms transverse beam size. Figure 2(b) shows an example of the focusing wakefield experienced by the beam (laser-beam parameters given in the caption of Fig. 2). In this example, the beam has an energy $\gamma = 10^4$, normalized transverse size $\sigma_r = 0.25$, and normalized emittance $\epsilon_n = 0.03$ (for example, $\epsilon_n = 0.5$ μm for a wall density of $n_w = 10^{17}$ cm^{-3}). The focusing wakefield is shown at two phases (near the beam head $\zeta = -3.6$ and near the beam tail $\zeta = -4.3$). The channel ions, with $n_c/n_w = 5 \times 10^{-5}$ in this example, provide matched beam propagation throughout the electron beam.

Positron beams can be accelerated in a similar fashion as electrons using a ramped or trapezoidal beam distribution, as described in Sec. II C, with $\varphi = \Omega\zeta_{\rm head}$ being the phase shift of the head of the positron beam with respect to the peak accelerating field for positrons. Although a near-hollow plasma channel can be effective in providing uniform, controlled focusing for electron beams, such a channel would provide a defocusing force to a positron beam. For a relativistic positron beam one would operate using a hollow plasma channel ($n_c = 0$), and rely on external focusing. Strong focusing could be achieved by using permanent magnetic quadrupoles positioned around the plasma channel structure.

IV. SUMMARY AND CONCLUSIONS

In this work we have examined beam-loading in laser-plasma accelerators using a near-hollow plasma channel. In this near-hollow plasma channel geometry, the accelerating fields are determined by the wall density, whereas the channel density may be used to independently control the focusing fields experienced by an electron beam. The focusing fields from the channel ions are linear in radial position and uniform in wakefield phase, eliminating any emittance growth due to beam mismatch.[20] In addition, by controlling the focusing force in this manner, the beam density can be controlled, eliminating any ion motion in the channel.[21] The near-hollow plasma channel geometry considered in this work effectively eliminates emittance growth from Coulomb scattering.[13]

The wakefields in a near-hollow plasma channel, excited by a drive laser and a witness particle beam, were computed. The guiding condition for a Gaussian laser driver propagating in a near-hollow channel was calculated [cf. Eq. (7)]. Triangular and trapezoidal current distributions were considered to eliminate head-to-tail differences in the accelerating field throughout the beam. By properly shaping and phasing the beam in the laser-driven wakefield, high-gradient acceleration can be achieved with high efficiency, and without induced energy spread. The laser-driven electrostatic wake (in the wall plasma) results in reduced efficiency, although efficiency may be improved by transverse shaping of the laser pulse so that only the electromagnetic mode is excited. For the numerical example presented in Sec. II C at $n_w = 10^{17}$ cm^{-3}, an accelerating gradient of 2.3 GV/m was generated with 73% efficiency of energy transfer from the laser-driven wakefield to the beam. In addition, short beams (compared to the skin depth of the wall density) can be accelerated without energy

spread and with high efficiency and accelerating gradient using trapezoidal shaped bunches in a multiple bunch train format.

Both electron and positron beams can be accelerated in this plasma channel geometry. A positron beam may be accelerated with high efficiency, without energy spread growth, in a similar fashion as an electron beam. Matched propagation of a positron beam can be achieved using a hollow channel with external focusing (generated by, for example, permanent magnetic quadrupoles). Although we have focused on laser drivers for excitation of the accelerating wakefield, the beam-loading analysis presented also applies to particle beam drivers.

In this work we have assumed a linear plasma response $|E_z| < E_w$. In particular, the accelerating gradients (and accelerated charge) can be increased by increasing the drive laser intensity. However, a nonlinear analysis and numerical modeling are then required to determine the optimal beam loading, and non-ideal effects, such as wall motion, need to be considered. The effects of slippage between the driver and witness bunch were also neglected in this work. Tapering the plasma density may be considered to control slippage.[22,23]

The proposed approach of using shaped beams in a near-hollow plasma channel geometry enables efficient acceleration while preserving high-quality electron and positron beams in plasma-based accelerators for high-energy physics applications.

ACKNOWLEDGMENTS

This work was supported by the Director, Office of Science, Office of High Energy Physics, of the U.S. Department of Energy under Contract No. DE-AC02-05CH11231.

Appendix A: Wakefield excitation

In this Appendix we present the solution for the linear wakefields in a near-hollow channel driven by a laser and/or charged particle beam and calculate the total energy deposited in the plasma channel. The excited wakefield can be derived from Maxwell equations and the linearized fluid equations for a cold, collisionless plasma, assuming a quasi-static driver. The linearized plasma electron fluid momentum equation is

$$4\pi\partial_t \boldsymbol{J}_p = k_p^2 \left[\boldsymbol{E} + (m_e c^2/e)\nabla a^2/4\right], \tag{A1}$$

where $\boldsymbol{J}_p$ is the plasma current, $k_p^2 = 4\pi e^2 n(r)/m_e c^2$, and $m_e c^2 \nabla a^2/4$ is the laser ponderomotive force (assuming linear polarization of the laser). Combining Eq. (A1) with the Maxwell equations yields

$$\nabla \times (\nabla \times \boldsymbol{E}) + \left(\partial_t^2 + k_p^2\right) \boldsymbol{E} = -k_p^2 (m_e c^2/e) \nabla a^2/4 - 4\pi \partial_t \boldsymbol{J}_b, \tag{A2}$$

where $\boldsymbol{J}_b$ is the particle beam current. In the following, the fields are normalized to $E_w = m_e c^2 k_w/e$ and the length scales to k_w^{-1}.

In the channel ($r < r_c$), $k_p^2 = k_c^2$ (plasma electrons in the near-hollow channel are assumed to be expelled, $k_c^2 \ll 1$, leaving ion density n_c), and the Poisson equation is

$$\nabla \cdot \boldsymbol{E} \simeq (q/e) k_b^2 + k_c^2, \tag{A3}$$

where $k_b^2 = 4\pi e^2 n_b(\zeta, r)/m_e c^2$ is the beam density with q the charge of the beam particles. In the wall plasma ($r > r_b$), $k_b^2 = 0$, $k_p^2 = 1$, and the plasma fluid continuity equation and the Poisson equation may be combined to yield

$$\left(\frac{\partial^2}{c^2 \partial t^2} + 1\right) \nabla \cdot \boldsymbol{E} = -\nabla^2 a^2/4. \tag{A4}$$

With the quasi-static approximation such that the wakefields and drivers are a function of the co-moving variable $\zeta = z - c\beta_p t$, with $\beta_p \simeq 1$, a Fourier transform $\boldsymbol{E}(\zeta, r) \to \tilde{\boldsymbol{E}}(k, r)$ may be applied. Solving Eqs. (A2) and (A3) for the wakefields in the channel ($r < r_c$) yields

$$\tilde{E}_z = C_1, \tag{A5}$$

$$\tilde{E}_r = -ikC_1 \frac{r}{2} + \frac{2}{r} \frac{\tilde{I}}{I_A} + 2\pi \delta(k) k_c^2 r/2, \tag{A6}$$

and $\tilde{B}_\theta = \tilde{E}_r - \partial_r \tilde{E}_z/ik = \tilde{E}_r$, where I is the beam current and $I_A = m_e c^3/e$. In the wall ($r > r_c$), assuming vanishing fields at $r \to \infty$, Eqs. (A2) and (A4) may be solved for the wakefields,

$$\tilde{E}_z = C_2 K_0(r) - \frac{ik\tilde{a}^2/4}{1 - k^2}, \tag{A7}$$

$$\tilde{E}_r = ikC_2 K_1(r) - \frac{\partial_r \tilde{a}^2/4}{1 - k^2}, \tag{A8}$$

and $\tilde{B}_\theta = \tilde{E}_r - \partial_r \tilde{E}_z/(ik)$, where K_0 and K_1 are modified Bessel functions. Here C_1 and C_2 are constants determined by the boundary conditions: $E_z|_{r_c} = 0$, $B_\theta|_{r_c} = 0$, and

$$\left[(k^2 - k_p^2)\tilde{E}_r - k_p^2 \partial_r \tilde{a}^2/4\right]_{r_c} = 0. \tag{A9}$$

Applying the boundary conditions yields

$$C_1 = \frac{-ik\Omega^2}{k^2-\Omega^2}\left[W_0\frac{\tilde{I}}{I_A} - \frac{\tilde{a}^2(r_c)}{4}\right], \tag{A10}$$

$$C_2 = \frac{-ik\Omega^2}{k^2-\Omega^2}\left[W_0\frac{\tilde{I}}{I_A} - \frac{\tilde{a}^2(r_c)}{4}\right]\frac{1}{K_0(r_c)} + \frac{ik}{1-k^2}\frac{\tilde{a}^2(r_c)}{4K_0(r_c)}, \tag{A11}$$

where

$$W_0 = \frac{2K_0(r_c)}{r_cK_1(r_c)}, \tag{A12}$$

and

$$\Omega = \left[1 + \frac{r_cK_0(r_c)}{2K_1(r_c)}\right]^{-1/2} \tag{A13}$$

is the excited mode wavenumber.

Taking the inverse Fourier transform yields

$$E_z = -\Omega^2\int_\infty^\zeta d\zeta' \cos[\Omega(\zeta-\zeta')]\left[\frac{a^2(r_c,\zeta')}{4} - W_0\frac{I(\zeta')}{I_A}\right] \tag{A14}$$

in the channel ($r < r_c$), and

$$E_z = -\int_\infty^\zeta d\zeta' \cos(\zeta-\zeta')\frac{a^2(r_c,\zeta')}{4}\left[\frac{a^2(r)}{a^2(r_c)} - \frac{K_0(r)}{K_0(r_c)}\right] - \Omega^2\frac{K_0(r)}{K_0(r_c)}\int_\infty^\zeta d\zeta' \cos[\Omega(\zeta-\zeta')]\left[\frac{a^2(r_c,\zeta')}{4} - W_0\frac{I(\zeta')}{I_A}\right] \tag{A15}$$

in the wall ($r > r_c$). The excited mode in the channel Eq. (A14) is electromagnetic, with frequency $\Omega k_w c$, whereas the field in the wall Eq. (A15) has an electrostatic component [first integral on the right-hand side of Eq. (A15) with oscillation frequency equal to the plasma frequency in the wall $k_w c$] and an electromagnetic component [second integral on the right-hand side of Eq. (A15) with frequency $\Omega k_w c$]. The relativistic particle beam with current I will only excite an electromagnetic mode, whereas the laser drives both modes. As indicated by Eq. (A15), if the laser has the transverse profile $a^2(r) = a^2(r_c)K_0(r)/K_0(r_c)$ for $r > r_c$, the laser will only excite the electromagnetic mode.

1. Electromagnetic mode

The electromagnetic fields excited behind the driver have the form

$$E_z = A_0 \cos(\Omega\zeta), \tag{A16}$$

$$E_r = A_0 \sin(\Omega\zeta)\Omega r/2, \tag{A17}$$

$$B_\theta = E_r, \tag{A18}$$

in the channel ($r < r_c$), and

$$E_z = A_0 \frac{K_0(r)}{K_0(r_c)} \cos(\Omega\zeta), \tag{A19}$$

$$E_r = -A_0\Omega \frac{K_1(r)}{K_0(r_c)} \sin(\Omega\zeta), \tag{A20}$$

$$B_\theta = (1 - \Omega^{-2})E_r, \tag{A21}$$

in the wall ($r > r_c$), where A_0 is the peak amplitude of the accelerating field given by the integral Eq. (A14). For a bi-Gaussian laser profile with envelope

$$a^2 = a_0^2 \exp(-\zeta^2/2L^2) \exp(-2r^2/w_0^2), \tag{A22}$$

where L is the rms intensity pulse length and w_0 the laser spot size, the wake amplitude behind the laser is

$$A_0 = a_0^2(\pi/8)^{1/2}\Omega^2 L e^{-(\Omega L)^2/2} e^{-2r_c^2/w_0^2}, \tag{A23}$$

and with pulse duration $L = \Omega^{-1}$ the wake amplitude is maximum $A_0 \simeq 0.38\Omega a_0^2 \exp(-2r_c^2/w_0^2)$.

The energy per unit length in the electromagnetic mode[11] is the sum of the energy in the fields and the plasma fluid motion,

$$\begin{aligned} U_{\rm em} &= \int d^2r_\perp \left(u_{\rm field} + u_{\rm fluid}\right) \\ &= \int_0^\infty r dr \frac{1}{8}\left[E_z^2 + (E_r - B_\theta)^2 + \Omega^{-2}(E_z^2 + E_r^2)\right] \\ &= A_0^2 \left[\frac{r_c K_1(r_c)}{4\Omega^2 K_0(r_c)}\right]. \end{aligned} \tag{A24}$$

2. Electrostatic mode

The electrostatic fields in the channel $r < r_c$ have the form

$$E_r = k_c^2 r/2, \tag{A25}$$

and in the wall $r > r_c$ the laser-driven electrostatic fields have the form

$$E_z = A_1 \cos(\zeta) \left[\frac{a^2(r)}{a^2(r_c)} - \frac{K_0(r)}{K_0(r_c)} \right], \tag{A26}$$

$$E_r = A_1 \sin(\zeta) \left[\frac{\partial_r a^2(r)}{a^2(r_c)} + \frac{K_1(r)}{K_0(r_c)} \right], \tag{A27}$$

where A_1 is given by the integral

$$E_z = -\int_\infty^\zeta d\zeta' \cos(\zeta - \zeta') \frac{a^2(r_c, \zeta')}{4} \left[\frac{a^2(r)}{a^2(r_c)} - \frac{K_0(r)}{K_0(r_c)} \right]. \tag{A28}$$

For a bi-Gaussian laser profile, Eq. (A22),

$$A_1 = a_0^2 (\pi/8)^{1/2} L e^{-L^2/2} e^{-2r_c^2/w_0^2}, \tag{A29}$$

and for a laser pulse duration that is resonant with the electromagnetic mode $\Omega L = 1$,

$$A_1/A_0 = \Omega^{-2} e^{(1-\Omega^{-2})/2}. \tag{A30}$$

The energy per unit length in the electrostatic mode is

$$U_{\rm es} = \int d^2 r_\perp \left(u_{\rm field} + u_{\rm fluid} \right) = \frac{(k_c r_c)^4}{64} + \frac{A_1^2}{4} \int_{r_c}^\infty r dr \left\{ \left[\frac{a^2(r)}{a^2(r_c)} - \frac{K_0(r)}{K_0(r_c)} \right]^2 + \left[\frac{\partial_r a^2(r)}{a^2(r_c)} + \frac{K_1(r)}{K_0(r_c)} \right]^2 \right\}. \tag{A31}$$

For $k_c r_c \ll 1$, the energy in the electrostatic fields is dominated by the fluid motion in the wall plasma $r > r_c$ excited by the laser ponderomotive force. The total energy per unit length deposited in the plasma channel by the driver is $U_{\rm em} + U_{\rm es}$.

REFERENCES

[1] E. Esarey, C. B. Schroeder, and W. P. Leemans, Rev. Mod. Phys. **81**, 1229 (2009).

[2] P. Chen, J. M. Dawson, R. W. Huff, and T. Katsouleas, Phys. Rev. Lett. **54**, 693 (1985).

[3] J. B. Rosenzweig, Phys. Rev. A **38**, 3634 (1988).

[4] W. P. Leemans, B. Nagler, A. J. Gonsalves, C. Tóth, K. Nakamura, C. G. R. Geddes, E. Esarey, C. B. Schroeder, and S. M. Hooker, Nature Phys. **2**, 696 (2006).

[5] I. Blumenfeld, C. E. Clayton, F.-J. Decker, M. J. Hogan, C. Huang, R. Ischebeck, R. Iverson, C. Joshi, T. Katsouleas, N. Kirby, W. Lu, K. A. Marsh, W. B. Mori, P. Muggli, E. Oz, R. H. Siemann, D. Walz, and M. Zhou, Nature **445**, 741 (2007).

[6]B. E. Blue, C. E. Clayton, C. L. O'Connell, F.-J. Decker, M. J. Hogan, C. Huang, R. Iverson, C. Joshi, T. C. Katsouleas, W. Lu, K. A. Marsh, W. B. Mori, P. Muggli, R. Siemann, and D. Walz, Phys. Rev. Lett. **90**, 214801 (2003).

[7]A. Seryi, M. J. Hogan, S. Pei, T. O. Raubenheimer, P. Tenenbaum, C. Huang, C. Joshi, W. Mori, T. Katsouleas, and P. Muggli, in *Proc. PAC09* (JACoW, Vancouver, BC, 2009); E. Adli, J. P. Delahaye, S. J. Gessner, M. J. Hogan, T. Raubenheimer, W. An, C. Joshi, and W.Mori, "A Beam Driven Plasma-Wakefield Linear Collider: From Higgs Factory to Multi-TeV," Tech. Rep. SLAC-PUB-15426 (SLAC, 2013).

[8]C. B. Schroeder, E. Esarey, C. G. R. Geddes, C. Benedetti, and W. P. Leemans, Phys. Rev. ST Accel. Beams **13**, 101301 (2010); C. B. Schroeder, E. Esarey, and W. P. Leemans, *ibid.* **15**, 051301 (2012).

[9]T. C. Chiou, T. Katsouleas, C. Decker, W. B. Mori, G. Shvets, and J. S. Wurtele, Phys. Plasmas **2**, 310 (1995).

[10]T. C. Chiou and T. Katsouleas, Phys. Rev. Lett. **81**, 3411 (1998).

[11]C. B. Schroeder, D. H. Whittum, and J. S. Wurtele, Phys. Rev. Lett. **82**, 1177 (1999).

[12]W. D. Kimura, H. M. Milchberg, P. Muggli, X. Li, and W. B. Mori, Phys. Rev. ST Accel. Beams **14**, 041301 (2011).

[13]C. B. Schroeder, E. Esarey, C. Benedetti, and W. P. Leemans, Phys. Plasmas **20**, 080701 (2013).

[14]S. van der Meer, "Improving the power efficiency of the plasma wakefield accelerator," CLIC Note 3, CERN/PS/85-65 (CERN, Geneva, Switzerland, 1985).

[15]T. Katsouleas, S. Wilks, P. Chen, J. M. Dawson, and J. J. Su, Part. Accel. **22**, 81 (1987); S. Wilks, T. Katsouleas, J. M. Dawson, P. Chen, and J. J. Su, IEEE Trans. Plasma Sci. **PS-15**, 210 (1987).

[16]M. Tzoufras, W. Lu, F. S. Tsung, C. Huang, W. B. Mori, T. Katsouleas, J. Vieira, R. A. Fonseca, and L. O. Silva, Phys. Rev. Lett. **101**, 145002 (2008); Physics of Plasmas **16**, 056705 (2009).

[17]G. Shvets, J. S. Wurtele, T. C. Chiou, and T. C. Katsouleas, IEEE Trans. Plasma Sci. **24**, 351 (1996); G. Shvets and X. Li, Phys. Plasmas **6**, 591 (1999).

[18]C. Benedetti, C. B. Schroeder, E. Esarey, and W. P. Leemans, Phys. Plasmas **19**, 053101 (2012).

[19]C. Benedetti, C. B. Schroeder, E. Esarey, C. G. R. Geddes, and W. P. Leemans, in *Proc.*

of 2010 Advanced Accelerator Concepts Workshop, Vol. 1299, edited by G. Nusinovich and S. Gold (AIP, NY, 2010) pp. 250–255; C. Benedetti, E. Esarey, W. P. Leemans, and C. B. Schroeder, in *Proc. of ICAP2012* (2012) p. THAAI2.

[20]A. G. Khachatryan, A. Irman, F. A. van Goor, and K.-J. Boller, Phys. Rev. ST Accel. Beams **10**, 121301 (2007); T. Mehrling, J. Grebenyuk, F. S. Tsung, K. Floettmann, and J. Osterhoff, **15**, 111303 (2012).

[21]J. B. Rosenzweig, A. M. Cook, A. Scott, M. C. Thompson, and R. B. Yoder, Phys. Rev. Lett. **95**, 195002 (2005).

[22]T. Katsouleas, Phys. Rev. A **33**, 2056 (1986).

[23]W. Rittershofer, C. B. Schroeder, E. Esarey, F. J. Grüner, and W. P. Leemans, Phys. Plasmas **17**, 063104 (2010).